Journal of Alloys and Compounds, *188* (1992) 147–151
JALCOM 9020

Characterization of zones resulting from the action of carbon dioxide laser impacts on dentinal hydroxyapatite

G. Marcon and B. Vidal
Institut National Polytechnique, LTPCM/ENSEEG, Domaine Universitaire, BP 75 38402 Saint Martin-d'Hères (France)

Abstract

In spite of the reasonably large number of works relating to CO_2 laser irradiation of teeth, the effects of power level and impact time on dentine have not yet been analysed in detail, in particular the effects of power level on the development of microcracks and the blocking phenomenon of tubules. For this purpose, thermal effects were investigated by single and multiple impacts on dentinal hydroxyapatite. Results obtained from numerous samples show that laser irradiation may produce deep craters, the size of which depends on the power level and duration of the laser beam. The craters thus formed are composed of three distinct heat-affected zones. Formation of the craters is accompanied by the development of microcracks in the heat-affected zones as well as in the non-affected region surrounding the craters. Compositional, phase and structural changes are observed. An increase in hardness and the blocking of dentinal tubules in the thermal-affected zone were detected.

1. Introduction

The sterilizing effect [1, 2] and dentine–pulpar repairs [3–5] have been the subjects of most previous studies on the use of CO_2 laser beams for dental applications. The resulting heat-effects will be different for enamel (hard tissue) [6, 7] and dentine (hydrated half-hard tissue) [3, 8–12]. However, all authors showed the formation of craters, made up of different zones, from which many microcracks originated.

In this paper, the thermal effect of CO_2 laser beams on the dentine of human teeth is described. We investigated single and multiple impacts. We show that craters are formed, the size of which increases with power level and duration of the CO_2 laser beam. Around the craters are three very different zones with microcracks extending towards non-irradiated dentine. The number and size of the microcracks depend closely on the laser operating parameters.

The objective of this work was to determine accurately the compositional, structural and phase changes of dentinal hydroxyapatite by identifying the phases resulting from transformation of the dentine and then studying the phenomenon of blocking of the tubules.

2. Experimental procedures

These studies were restricted to the dentine in human teeth which had been extracted and then kept in a physiological salt solution. After extraction the teeth were cut along a section perpendicular to their axis to remove the upper part. In a second stage, the tooth surface thus displayed was exposed to single or multiple impacts of a CO_2 laser beam. The laser used was a CO_2 surgical laser, Sharplan type ($\lambda = 10.6$ μm), emitting a beam of variable power ranging from 1 to 20 W, and energy density from 100 to 2000 J cm^{-2}. The focal length was 125 mm. The analysis techniques used were optical microscopy, scanning electron microscopy, electron microprobe analysis, X-ray analysis and microhardness (Knoop) measurements.

3. Experimental results

3.1. Observation of effects of single impacts

The impact of the laser on dentine creates a crater, the diameter and depth of which depend closely on the power level and the irradiation time (Fig. 1). We observe the formation of three distinct heat-affected zones with very different colour and structure (Fig. 2). The first zone of melted material appears white on the surface of the crater; this is the molten zone (MZ). The second zone appears in the subsurface and is black and charred; this is the carbonized zone (CZ). The third zone is opaque and whiter than the non-affected dentine; this is the denatured zone (DZ), which is further away from the crater. Figure 3 shows the centre cross-section of a crater.

3.2. The different zones

On the surface of the crater we can see one zone, the depth of which ranges from 10 to 50 μm, resulting from

0925-8388/92/$5.00

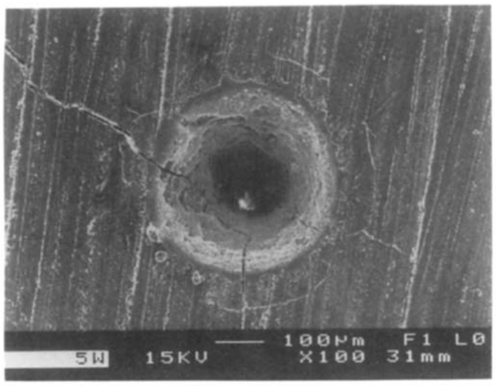

Fig. 1. Scanning electron micrograph of a single laser impact (5 W, 0.05 s).

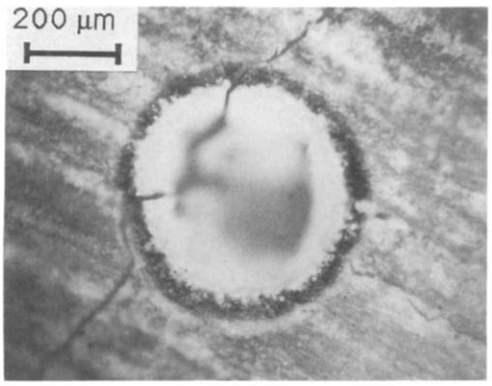

Fig. 2. Optical micrograph of a single laser impact (15 W, 0.05 s). The three different zones around the crater are visible.

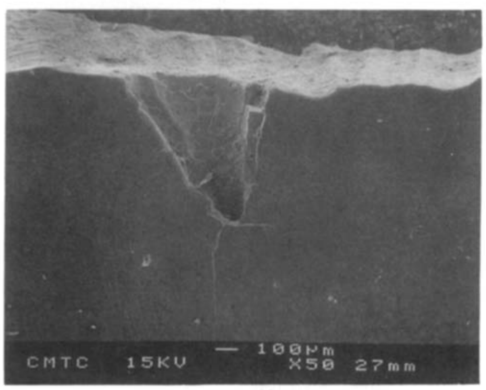

Fig. 3. Scanning electron micrograph of a single laser impact in a centre cross-section parallel to the laser beam axis (5 W, 0.05 s).

solidification which follows melting of the hydroxyapatite, vaporization of water and volatilization of the organic components of the dentine. This MZ has a smooth aspect at the top of the crater but is thinner and rougher at the bottom. The hydroxyapatite melted by the laser impact has been pushed out towards the top by the gas resulting from the decomposition of organic

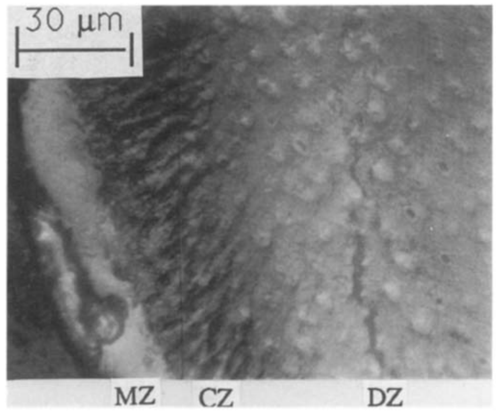

Fig. 4. Optical micrograph showing the different zones (20 W, 0.05 s): MZ (molten zone), CZ (carbonized zone), DZ (denatured zone).

components and steam. However, the molten hydroxyapatite from the middle of the crater has coated the side of the crater and solidified at the bottom. This phenomenon shows the characteristics of the plasma effect, and in fact the size and the shape of the crater depend on the power level and exposure time. The higher the power level or the longer the exposure, the bigger will be the plasma effect.

This zone consists of molten dentine, and appears heavily modified when compared with the structure of normal dentine. The MZ rests on the CZ without any transitional junction zone (Fig. 4). On the surface of the MZ, we can observe numerous micropores, as well as crystals ranging in length from 30 to 40 µm, particularly for the low power level cases. This indicates a partially crystallized state within the MZ. In fact, it seems that in certain places such crystals coexist with an amorphous matrix. We have not been able to determine a general rule for solidification, but we can say that the crystallized areas of the MZ are located at the top part of the crater for the high power level cases. In all cases we can observe amorphous solidified drop-like particles at the bottom of the crater. In cross-section the MZ seems to be composed of fine pores lying in the same direction, thus allowing the gas to escape from the two other heat-affected zones. This explains the microporosities which are seen on the surface. These channels are apparently formed between more or less parallel rod-like shapes and perpendicular to the wall of the crater. These rods of size 1 µm correspond to the depth of the MZ. They seem to have the same origin as those observed at the surface of the crater in low power level cases. This crystal growth occurs perpendicular to the different isotherms as a result of thermal propagation in the dentine in the same way as columnar crystal growth.

The difference between the two other zones is not clearly shown by scanning electron microscopy, in contrast to the preceding MZ which appears heavily modified. These two zones retain the dentine structure. The transition between the MZ and the CZ is very rough. As we can see in Fig. 4, the CZ is in most cases pervaded by porosities lying in the same direction which allow gas (CO_2, H_2O), resulting from the thermal effects, to escape. The transition between the CZ and the next DZ is very progressive. Using a stereoscopic optical microscope, we often observe a darkish zone between the CZ and the DZ. This darkish zone seems to be a transition zone. The tubules appear to be sealed along the whole depth of this thermal-affected zone (TAZ, CZ and DZ), *i.e.* about 75 μm (40 μm for the CZ and 35 μm for DZ). This phenomenon was observed in 70% of cases. The difference between this TAZ and the non-affected dentine on the same sample is obvious in most cases. This result arises from the laser thermal effect. It can be obtained regardless of the orientation of the tubules relative to the considered section. This phenomenon is especially well defined when the tubules are perpendicular to the crater wall.

In 30% of cases we cannot be sure whether tubules were sealed or not. In these cases, the samples contained very small tubules that were difficult to distinguish. After polishing, tubules can be seen in relief as a result of the denatured intertubular dentine being removed by the polishing apparatus. This peculiarity occurs in every case, and we can therefore infer that the dentine of the DZ is weakened compared with the normal dentine in a large part of the DZ. This phenomenon does not appear in the carbonized zone.

We have noticed that some tubules are sometimes unblocked at the MZ–CZ junction. This happens where tubules reach the surface of the treated dentine. These unblocked tubules permit the escape of gas resulting from thermal effects. In addition, a few microcracks were observed in the MZ extending from its surface towards the CZ (Fig. 2). At the CZ–DZ junction as in the DZ, these microfissures can extend in a circular way surrounding the crater area (Figs. 1 and 4). They disrupt the CZ–DZ junction. Numerous microcracks were observed in most cases at the bottom of the crater. These microcracks extend through the tooth along the crater axis (see Fig. 3).

3.3. Observation of effects of multiple impacts

For this treatment, we observe a very important TAZ. In particular, in this TAZ, sealed tubules are visible between two craters (Fig. 5). This is due to overlapping of the two thermal spreading areas. In addition, we observe a large number of microcracks joining together between the craters, even for low power levels (Fig. 6). Teeth exposed to continuous laser irradiation have this effect enhanced.

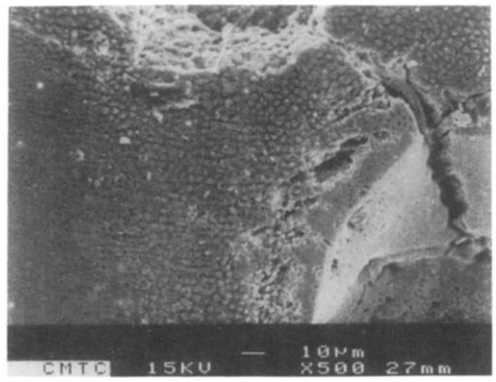

Fig. 5. Scanning electron micrograph showing spreading of the thermal affected zone between two craters. In this zone sealed tubules are visible.

3.4. Influence of power

The higher the power level or exposure, the greater is the volatilized dentine or crater volume (Fig. 7). As Melcer observed [3], the volume of volatilized dentine V is proportional to the power level W and impact time t. From the results in Fig. 8, the following relation is found: $V(\text{cm}^3) = 5.6 \times 10^{-5}\ W(\text{W})t(\text{s})$. We verified that the depth of the MZ increases with power level or impact time, while the depths of the CZ and DZ remain approximately constant (Table 1). Moreover, we observed that the bottom fissures decrease with power level and disappear for levels under 5 W. In contrast, circular microcracks always exist as well as in the MZ. If the beam power is decreased, the damage to the surrounding unaffected dentine area decreases.

3.5. Thermally induced structural changes

In order to obtain comparative results on structural changes, the enamel, dentine and MZ and CZ material were analysed by X-ray diffraction analysis.

Results show a hexagonal crystallographic structure like that of hydroxyapatite ($Ca_{10}(PO_4)_6(OH)_2$), *i.e.* the same structure as enamel or dentine.

The compositional changes were investigated by microprobe analysis along a line joining two craters. If we consider a line joining a non-affected dentine area to a

TABLE 1. Crater diameter, depth and volume and depths of different zones for different laser beam power levels and constant impact time

Power (W) $t = 0.05$ s	Diameter (μm)	Depth (μm)	Volume (10^{-5} cm^3)	CZ (μm)	DZ (μm)
5	400	300	1.2	44	33
10	450	480	3.1	41	35
15	490	700	3.8	39	41
20	580	750	6.6	44	34

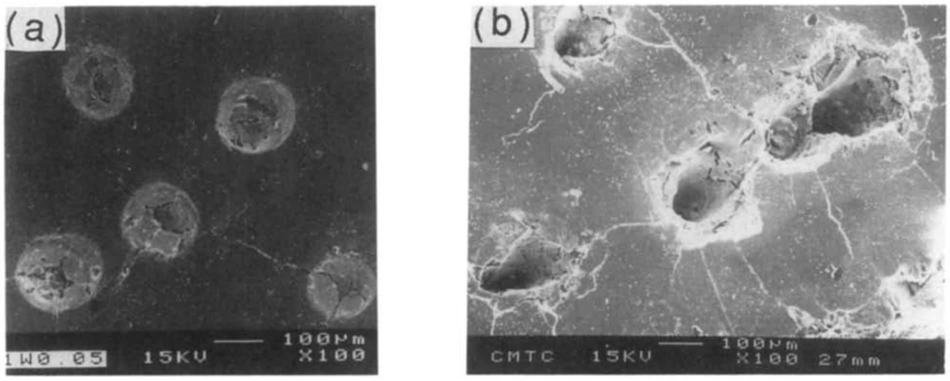

Fig. 6. Scanning electron micrographs of multiple laser impacts: (a) 1 W, 0.05 s; (b) 5 W, 0.05 s. For the lowest power, the attenuation of microcracks between craters is visible.

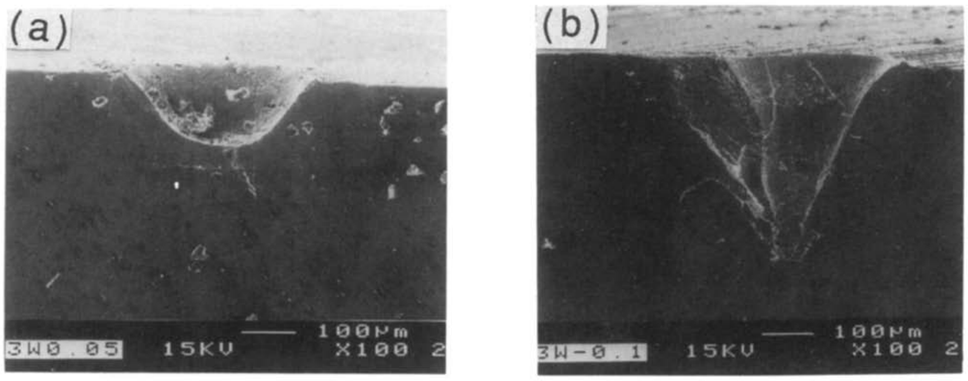

Fig. 7. Scanning electron micrographs showing the influence of laser beam impact time: (a) 3 W, 0.05 s; (b) 3 W, 0.1 s.

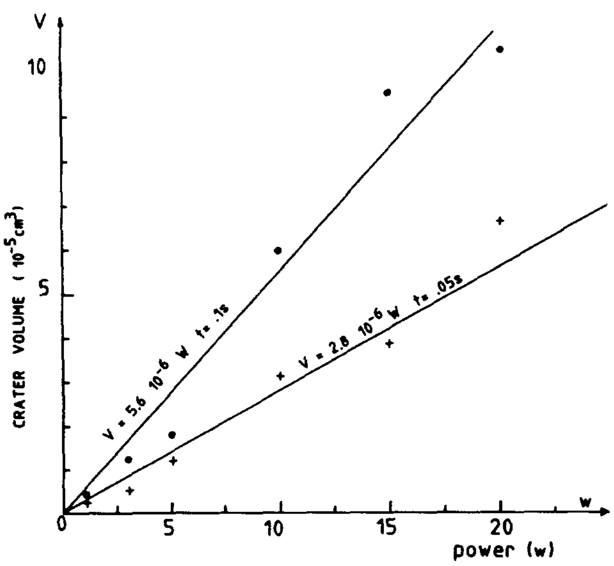

Fig. 8. Crater volume variation *vs.* laser beam power for two impact times.

crater for example, the calcium and phosphorus concentrations increase in the TAZ. This increase is more important between the CZ and MZ. We notice an average increase of 7% for calcium in the MZ compared with normal dentine, which can reach up to 15% or 20% for some samples. The magnesium concentration decreases in the DZ, increases up to its normal level in the CZ, and is higher in the MZ. The changes in oxygen concentration are similar to those of calcium and phosphorus. These results are similar to those of Kantola [13].

In fact, the laser beam power seems to influence the composition changes: the increase in calcium, phosphorus, and also oxygen reach maximum values in the TAZ when using a power level of 20 W.

In order to check for possible changes in hardness of irradiated dentine, the hardness was measured along lines perpendicular to the walls of the craters, on 20 differently treated teeth. Figure 9 shows an example of the variation in hardness, showing the relationship with the different zones. We can also see that the hardness of the MZ is nearly the same as the hardness of the enamel (hardness of enamel is in the range 200–320 HK, whereas that of the MZ ranges from 250 to 300 HK). This decreases steeply in the CZ although its value is higher than that of normal dentine (in the range 50–100 HK).

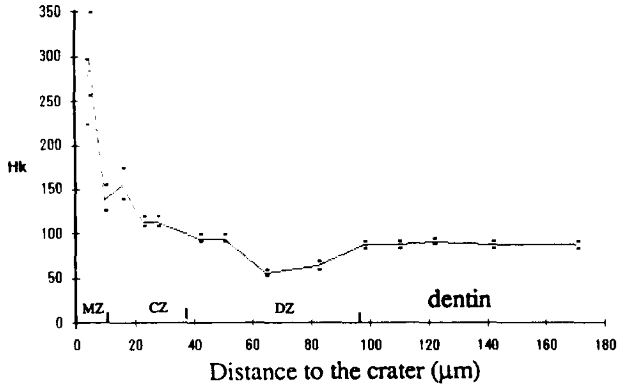

Fig. 9. Hardness variation along a cross-section perpendicular to the axis of a crater, relationship with the different zones (5 W, 0.05 s).

Generally, the limit of the DZ, more often corresponding to the transition zone with the CZ, is harder, but a weakened zone appears on many teeth when microcracks are present. This part of the DZ corresponds to the zone of spreading circular fissures as well as the zone of weakened intertubular dentine. It is worth noting, as Melcer observed [3], that the hardness of the MZ increases with the power level. The hardness of the TAZ is unchanged.

4. Conclusion

The effects of CO_2 laser on dentinal hydroxyapatite are as follows.

A crater is formed, the volume of which increases with laser beam power and impact time. A plasma effect occurs if the power level or exposure time are high. Microfissures appear at the bottom of the crater when power levels higher than 5 W are used.

A chalky, white molten zone 10–50 μm deep develops on the surface of the crater, the depth of which increases with power level. This zone consists of fused material, fused or partially recrystallized. At higher power levels, the molten zone contains parallel hydroxyapatite rolls. The concentrations of calcium, phosphorus and oxygen are higher than in normal dentine. It has the same appearance as enamel or synthetic apatite (hardness, composition, structure). This similarity is enhanced with power level. This zone is pervaded by microcracks whatever the power level. In most cases these microcracks extend through the non-affected dentine perpendicularly to the crater wall.

A black carbonized zone 40 μm deep develops, the depth being independent of the power used. This zone is in the subsurface of the molten zone; it shows a smaller degree of mineralization and contains less calcium and phosphorus than normal dentine. The junction with the molten zone has no transition zone. Its morphology is the same as that of normal dentine and its hardness is higher.

An opaque denatured zone 35 μm deep is created, the depth of which is independent of the power used. The junction with the former zone is very progressive. Tubules appear sealed in these two zones. Furthermore, numerous circular microfissures are observed at the junction of these two zones, especially in the denatured zone which seems to be weakened locally compared with normal dentine.

As a result, it is important in clinical practice to keep the power level and exposure of the laser beam to the minimum required in order to reduce the formation of microcracks.

Acknowledgments

The extracted and irradiated teeth were supplied by Drs. J. P. Brun and P. B. Tardieu (European Club of Odonto Stomatology, Grenoble, France).

References

1 J. Melcer, R. Lequercq, S. Zeboulon, F. Melcer, C. J. Soussy and J. Dejardin, *Innov. Tech. Biol. Med.*, *7* (1986) 237.
2 Ph. Bonin, J. P. Rocca, J. P. Duprez and R. Vincent, *Les Questions d'Odonto-Stomatologie*, *43* (1986) 295.
3 J. Melcer, *Thèse de doctorat d'état en odontologie*, Paris V, 1985.
4 J. Melcer, *Lasers Surg. Med.*, *4* (1984) 311.
5 R. Stern, J. Vahl and F. Sognnaes, *J. Dent. Res.*, *51* (1972) 445.
6 R. Merard, *Inf. Dent.*, *22* (1982) 2153.
7 R. R. Lobene and S. Fine, *J. Dent. Res.*, *4* (1968) 311.
8 F. Lhuisset, *Ligament 136* (2ème trimestre, 1980) 103.
9 F. Lhuisset, *Chir. Dent. Fr.*, *31* (1979) 37.
10 J. Vahl, *Caries. Res.*, *2* (1968) 10.
11 S. Kantola and A. Scheinin, *Acta Odont. Scand.*, *9* (1968) 37.
12 G. Glover-Bondeau, *Thèse 2ème cycle*, Université R. Descarte, 1983.
13 S. Kantola, *Acta Odont. Scand.*, *6* (1972) 113.